Undergraduate Review

Volume 7 Article 19

2011

Stable Isotopic Constraints of the Turpan Basin in Northwestern China

Allen J. Schaen

Stable Isotopic Constraints of the Turpan Basin in Northwestern China

Allen J. Schaen

Allen Schaen is a senior majoring in Earth Science with a concentration in Geology. This research began in the summer of 2010 as an Adrian Tinsley Program Summer Grant and was also supported by a Geological Society of America Northeast Section Student Research Grant. This work was present at the 2010 American Geophysical Union Meeting in San Francisco in December. Allen plans to go to graduate school for Geology in the fall of 2011.

Stable isotopic analysis of sedimentary rocks can be used to reconstruct past geologic changes in the elevation and climate of topographic features such as mountain ranges and plateaus. The Tibetan Plateau is an ideal field laboratory for conducting this type of study because of the Plateau's extreme topographic relief and relatively recent geologic growth. Here we present oxygen and carbon isotope compositions from a suite of sedimentary rock samples taken from the western Turpan Basin in northwestern China. This area of the basin collects sediment from weathering and erosion of the Bogda Shan located to the north. The goal of this study is to analyze changes in the stable isotope composition of rocks as a function of stratigraphic position to reconstruct paleoelevations and paleoclimates in this part of the Tibetan Plateau.

The sedimentary rock samples analyzed in this study are Late Jurassic to Neogene age and are primarily mudstone, siltstone, and fine sandstone along with lesser limestone. Samples were powdered and then dissolved with phosphoric acid at 72°C. The liberated CO_2 gas was then analyzed using a Finnigan Delta Plus XL mass spectrometer with a gasbench inlet system. Oxygen isotope values range from -13.72 to -1.62‰ (PDB) and exhibit a large scale trend to more negative values toward the top of the stratigraphic sequence. Superimposed on this large scale trend are systematic variations in isotopic composition as a function of age. The most positive $\delta^{18}O$ values occur at approximately 160, 115, 60, and 5 ma. Conversely, $\delta^{18}O$ minima are observed at 150, 90, and 40 ma. $\delta^{13}C$ values range from -10.69‰ to 1.40‰ (PDB). The most positive $\delta^{13}C$ values (-4.3 to 1.4) occur from 120-160 ma. Younger samples display small scale variations with age with notable $\delta^{13}C$ minima of -10.7, -14.7, and -7.6‰ at 108, 80, and 17 ma, respectively.

The alternating $\delta^{18}O$ and $\delta^{13}C$ signals during the Late Jurassic and Early Tertiary suggests a tectonic influence and could be a result of the inferred inception of the Turpan Basin in the Jurassic and the Tertiary collision between the Indian and Eurasian plates respectively. Where the $\delta^{18}O$ and $\delta^{13}C$ track together during the Late Cretaceous suggests that evaporative effects may have altered the isotope record which is consistent with the arid climate and high atmospheric P_{CO2} levels during the warm Mesozoic Era. Taking into account other possible influences on the isotopic record including detrital effects, diagensis, and evaporation, it is inferred that the primary isotope signals result from two separate tectonic events in the Late Jurassic and Early

Tertiary with changes in climate during Cretaceous dominating in between.

Introduction

Orogenic plateaus form at convergent plate boundaries which, according to tectonic theory, is where two tectonic plates collide uplifting a landmass that is high, vast, and flat. The topography of plateaus, because they are expansive (flat on top and abruptly high) can have profound effects on local and global climate as they control atmospheric circulation. They also offer the chance to study subsurface processes which help refine plate tectonic models. The debate over the geologic history of the Tibetan Plateau is centered on the timing of the collision between the Indian and Eurasian plates along with its uplift scenario: whether the whole plateau uplifted at once or gradually in a stepwise fashion. In order to better understand the tectonic and climate history of the Tibetan Plateau, this study will provide stable isotope data from the Turpan Basin (Fig. 1) that has been derived from detrital sedimentary rocks in order to determine paleoelevations of the adjacent Bogda Shan (Shan is a Chinese term for mountain).

Isotopes are atoms with the same atomic number but different mass numbers, meaning a different number of neutrons in the nucleus. Because oxygen-18 (^{18}O) is heavier than oxygen-16 (^{16}O), it is more likely to precipitate out of a rising air mass first. Thus, as an air mass travels over a topographic barrier (mountain range, plateau) it will be become progressively depleted in ^{18}O and more enriched in ^{16}O. This process is called isotope fractionation. The amount of ^{18}O and ^{16}O in precipitation is therefore a reflection of the amount of these isotopes in the air mass it was derived from and the fractionation effect. When this water flows into a sedimentary basin, carbonate minerals such as calcite ($CaCO_3$) crystallize and incorporate the oxygen isotopes from this ancient H_2O in their mineral structure. As this process occurs throughout geologic time, the sedimentary rocks deposited in the basin will contain a record of ancient ^{18}O values that have been preserved as the Bogda Shan were uplifted. A linear relationship exists between ^{18}O values and elevation worldwide (Poage et al., 2001). Therefore paleoelevations can be determined providing insight into the elevation history of the Bogda Shan and these paleoelevations can be compared with other studies throughout the plateau to delineate any patterns. This will help to distinguish between tectonic models in regards to the area adjacent to the Turpan Basin i.e., whether the Bogda Shan were uplifted as a result of the northward expansion of the Tibetan Plateau due to the Indian-Eurasian collision (Tapponnier et al., 2001), or if the Bogda Shan have been continuously deformed and uplifted as a result of collisions with microcontinents since the Paleozoic (Shao et al. 1999; Shao et al., 2001; Greene et al., 2001)

Previous paleoelevational studies along the Tibetan Plateau provide further insight into the design of its uplift history. From the Oiyug Basin in southern Tibet, paleoelevational studies have been conducted using flora preserved within its lacustrine deposits (Spicer et al., 2003). They estimate paleoelevations of 4650 ± 875 m with floral ages at approximately 15.1 Ma derived from volcanic ash that has been dated using radioactive isotopes. Other work in the Oiyug Basin has been conducted using pedogenic carbonates to estimate paleoelevations of approximately 5200 +1330/-630 m by 15 Ma (Currie et al., 2005). DeCelles et al. (2007) used stable isotopic data derived from paleosol carbonates and aquatic fossils to establish paleoelevations in the area of the Nima Basin along the southern margin of the Tibetan Plateau. They conclude that central Tibet was at an elevation of ~4500- 5000 m during the Late Oligocene. Rowley and Currie (2006) have conducted paleoelevational studies in the Lunpola Basin which is situated in central Tibet south of the Qaidam Basin. The Lunpola Basin consists of two main stratigraphic units: the Niubao Formation (Paleocene-Oligocene Age) and the Dingqing Formation (Miocene-Pliocene Age) (Rowley and Garzione, 2007). Rowley and Currie (2006) estimate paleoelevations from the Miocene Age middle Dingqing Formation using isotopic data derived from lacustrine marls and micritic limestones to be 4260 m +460/-560 m. They also report paleoelevational data from the late Eocene-Oligocene Niubao Formation using isotopic data gathered from lacustrine and paleosol carbonates to be 4050m +500/-600 m. These oxygen isotope estimates have led to the conclusion that the central Tibetan Plateau has exceeded 4000 m since 35± 5 Ma (Rowley and Currie 2006). Cyr et al. (2005) used oxygen and carbon isotopes along with Mg/Ca ratios to provide paleoelevation data from the Fenghuoshan Group of the Hoh Xil Basin located in north-central Tibet. They employ this combined technique on Eocene-Oligocene Age lacustrine carbonates to estimate that the Hoh Xil Basin was most likely lower than 2000 m in Eocene Time. This conclusion infers that the Hoh Xil Basin (presently 4700 m) has experienced rapid surface uplift (> 2700 m) since 39 Ma (Cyr et al., 2005). Kent-Corson et al. (2009) used stable isotopic data along with sedimentary techniques to constrain the evolution of climate and topography along the Altyn Tagh Fault south of the Tarim Basin in the northern margin of the Tibetan Plateau. Their data suggest that mountain building in this region began during early to middle Miocene time. When taken as a whole, these paleoelevational studies along the Tibetan Plateau support an uplift scenario of a northward expansion of mountain building through time. The goal of this study is to determine the climate/tectonic influences on the isotopic record of the Bogda Shan which will provide insight into its uplift history.

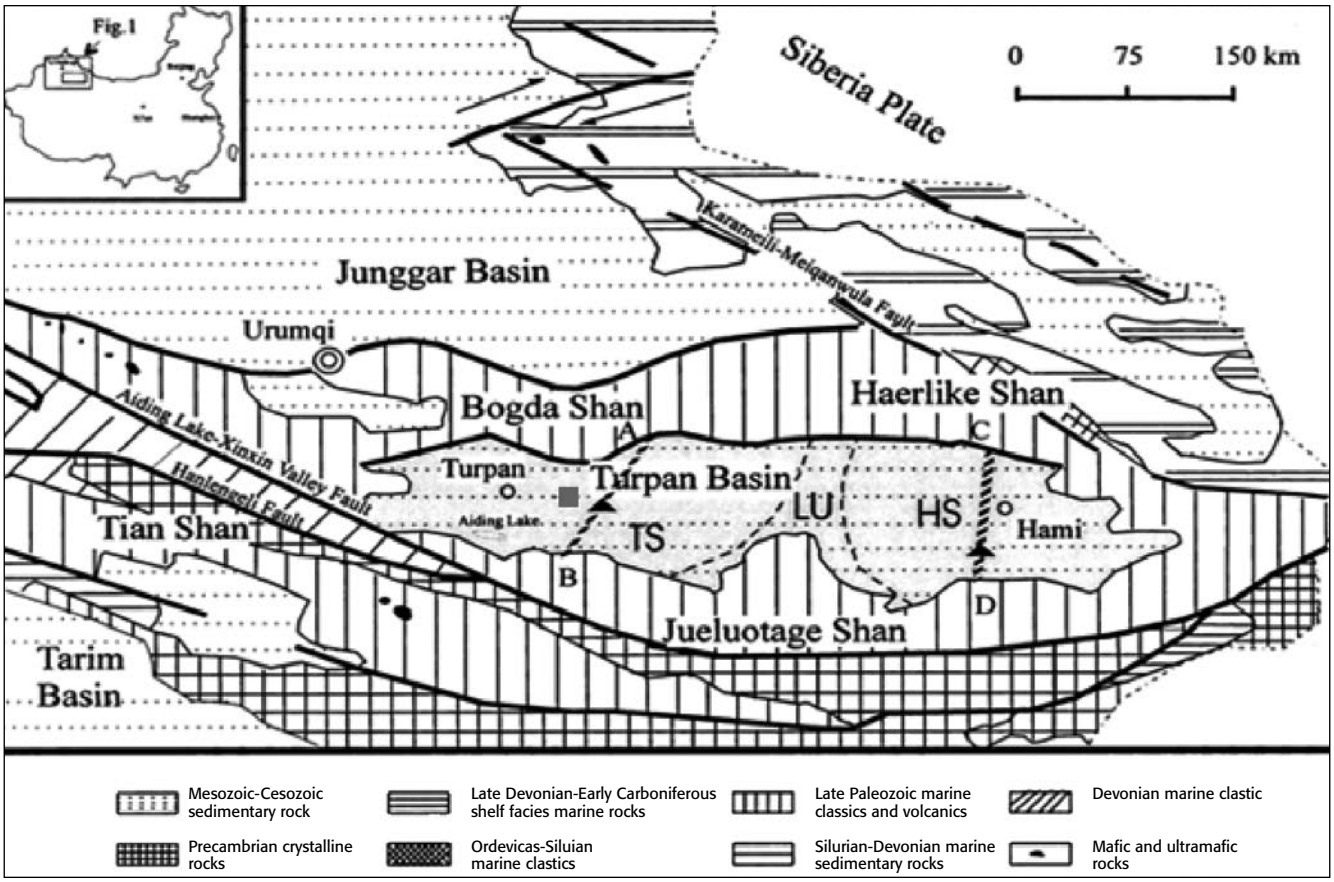

Figure 1: Geologic map of the Turpan Basin (NW China), red square indicates sample locality.

Geologic Background

The Turpan Basin is located in northwestern China in an area of complex and debated tectonic history. It is approximately 500 km long from east to west and 60-100 km wide from north to south, covering an area of 53,500 km^2 (Shao et al., 2001). The Turpan Basin is an intermontane basin bounded by the Bogda Shan to the north, the Haerlike Shan to the northeast and the Jueluotage Shan to the south, all of which are a part of the Tian Shan orogenic belt (Fig. 1). The Tarim Basin, separated by the Jueluotage Shan, is located to its southwest and the Junggar Basin, separated by the Bogda and Haerlike Shan, is located to its north. The Turpan Basin exhibits the second lowest surface elevation on Earth (-154 m) but is bounded on its northern flank by peaks as high as 5570 m in the Bogda Shan (Greene et al., 2001). The Bogda Shan is made up of Upper Carboniferous volcaniclastic and carbonate strata with some interbedded intermediate to felsic volcanic rocks, Permian continental clastic to pyroclastic rocks along with small amounts of limestone, and Triassic/Jurassic continental formations with coal seams (Shao et al. 1999). The Haerlike Shan, connected to the Bogda Shan from the east, consist of Devonian and Lower Carboniferous clastic to pyroclastic strata along with intermediate to felsic volcanic rocks that have undergone regional metamorphism (Shao et al. 1999). South of the Turpan, the Juueluotag Shan contains an array of Silurian, Devonian and Carboniferous metamorphosed volcanics (intermediate, felsic, pyroclastic), marine sedimentary strata, and plutonic igneous (ultramafic, mafic, intermediate/felsic) rock formations (Shao et al. 1999).

Due to central Asia's intricate tectonic setting of ancient ocean basins, collision zones, and fault systems, the interpretation of the tectonic and structural history of the Turpan Basin and its surrounding areas vary greatly. Some studies have used paleocurrent, sedimentary, and other stratigraphic data to suggest that the Turpan Basin was established by Early Jurassic time due to compressional uplift of the Bogda Shan (Hendrix et al., 1992; Shao et al., 1999; Shao et al., 2001; Greene et al., 2001). Others suggest that the Turpan Basin is an intermontane basin that formed in the Tian Shan orogenic belt during the Late Paleozoic (Cao, 1990). Still others consider that the Turpan basin was attached to the Junggar Basin prior to Late Permian time as a microcontinent (Hu et al., 1996; Ding et al., 1996). Some have used stratigraphy and volcanics to show that the Turpan Basin formed on oceanic crust (Carroll et al., 1990; 1991). Whether a combination or succession of some or all of these events took place is debated. Sandstone petrology and

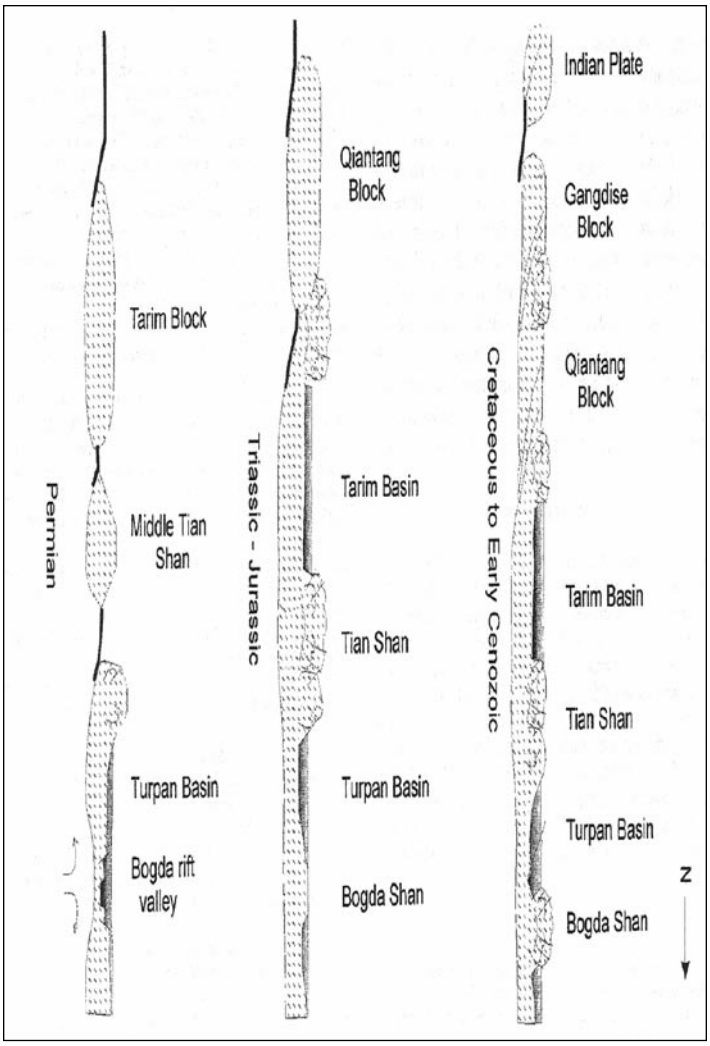

Figure 2: Cross section showing the inferred source regions for sedimentary rocks in the Turpan Basin as a function of time (Shao et al., 2001).

geochemistry has been used to break the tectonic evolution of the Turpan Basin, which is located in the Eurasian plate, into three stages (Shao et al., 2001). It is thought that Late Permian collision with the Tarim Block, a Triassic to Jurassic collision with the Qiangtang Block, and a Cretaceous to Tertiary collision with the Gangdise Block (Fig.2) has occurred in the past (Shao et al., 2001).

The Turpan Basin has been filled with more than 7000 m of continental sediment from the Late Permian to the late Tertiary (Shao et al., 1999). Starting in the Permian and continuing into the Mesozoic and Cenozoic, the Turpan's sedimentary environment changed from marine conditions to fluvial and lacustrine conditions (Zhu et al., 1988; Wu et al., 1997). The complex tectonic history of the Turpan Basin reflects its intricate sedimentary record, with changes from alluvial fan/fluvial conditions to lacustrine conditions between each sedimentary cycle separated by unconformities (Shao et al., 1999). The Upper Permian stratum consists of generally nonmarine deposits. The middle portion of the basin exhibits lacustrine deposits, whereas the northern and western sections contain alluvial and fluvial conglomerates that have formed from the underlying strata (Carroll et al., 1991). The Triassic strata for the most part consist of red conglomerates, coarse sandstone, and fine clastic sediments that contain coal and coal streaks deposited in an alluvial and lacustrine-fluvial environment (Shao et al., 1999). Shao et al. (1999) describe the Lower and Middle Jurassic stratigraphy of the Turpan Basin to be made up of green and gray clasts and coal that were deposited in a lacustrine-swamp environment. The Upper Jurassic stratum of the Turpan is made up of an array of coarse clastic rocks that were deposited in an arid climate in a plateau-fluvial depositional setting (Li, 1997a; Li, 1997b). Shao et al. 1999 interprets the presence of Late Jurassic red and red-purple sedimentary rocks to reflect a change in paleoclimate from arid to humid. They describe the angular unconformity that separates the Jurassic from the more localized Cretaceous age lacustrine sediments. The Tertiary stratum is more widely distributed than the Cretaceous strata throughout the basin. It consists of coarse clastic sediments in the lower part of the strata that were deposited in a braided fluvial/alluvial setting and fine clastic sediments that were deposited in a lacustrine environment in the upper part of the strata (Shao et al., 1999).

Methods

In 2003, a Stanford University sampling party made up of Bradley Ritts and Yongjun Yue collected sedimentary rock samples from the Turpan Basin south of the city of Urumqi where they keyed the samples into a stratigraphic section and recorded GPS coordinates. Fifty-five of these samples, labeled 03LQ110-03LQ163, from the Liamunqin section east of the city of Turpan (Fig. 1) were provided to me for analysis at Stanford University's Stable Isotope Biochemistry Laboratory. The samples are Late Jurassic to Neogene age fine grained sandstones, siltstones, mudstones and a single limestone. They range in color from red, brown, gray to green. I prepared the samples for analysis by powdering them using a Dremel tool and reacting them with acid to assess their carbonate content. These samples were analyzed for their ^{18}O and ^{13}C content using a Finnigan Delta Plus XL mass spectrometer with a gasbench inlet system. In the gasbench, the samples are placed in sealed containers and flushed with helium gas to purify the sample from the present atmosphere in the vial. They are then reacted with 100% phosphoric acid at 72°C where the sample dissolves, releasing the ancient CO_2 in its mineral structure. This CO_2 gas was sampled and moved to the mass spectrometer where ^{18}O, ^{16}O, ^{13}C, and ^{12}C are separated by mass, from which

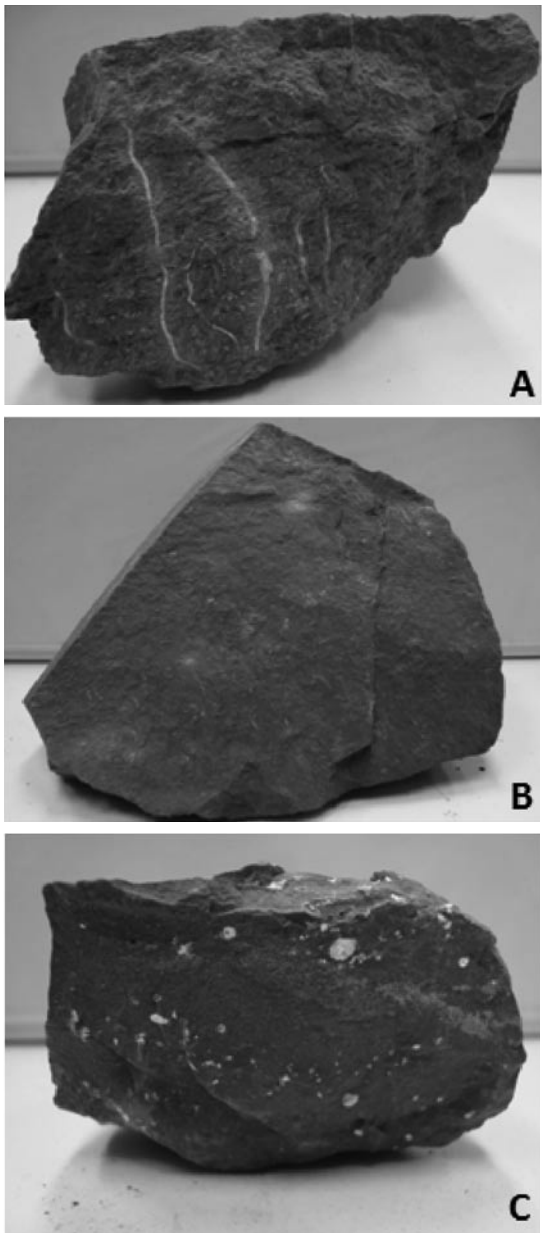

Figure 3: (A) Sample 03LQ137, red siltstone with root casts, (B) Sample 03LQ141, red siltstone with reduction spots, (C) Sample 03LQ140-2 red siltstone with carbonate nodules.

$\delta^{18}O$ and $\delta^{13}C$ values are calculated. The "δ" notation is used to describe the amount of a particular isotope in the sample in units of per mil (‰), relative to a measured standard. The standard employed in this study for all measurements is the Pee Dee Belemnite (PDB). Thus, a larger $\delta^{18}O$ value indicates relatively more ^{18}O in the sample compared to ^{16}O and a larger $\delta^{13}C$ value indicates more ^{13}C in the sample compared to ^{12}C, relative to PDB. All samples were slabbed in order to reveal any micromorphology present. When applicable, root casts, reduction spots, carbonate nodules and incipient carbonate pods were sampled and compared to the rest of the sample (Fig. 3).

Results

In stable isotopic analyses of 55 samples, oxygen isotope values range from -13.72‰ to -1.62‰. Late Jurassic samples exhibit oxygen isotope values ranging from -13.72‰ to -4.08‰. Late Jurassic or Cretaceous samples have oxygen values ranging from -10.59‰ to -7.78‰. Cretaceous samples have oxygen values ranging from -11.09 ‰ to -1.62‰. Late Cretaceous to Eocene samples have oxygen values ranging from -12.87‰ to -8.29‰. Neogene samples exhibit oxygen values from -11.54‰ to -8.89‰. Of the Late Cretaceous to Eocene samples that have micromorphology, two display more negative oxygen isotope signatures. The root casts taken from sample 03LQ137 have a $\delta^{18}O$ signature of -12.16‰. The carbonate nodules taken from sample 03LQ140-2 have a $\delta^{18}O$ signature of -16.42‰ exhibiting the most negative oxygen signature in the whole suite of rocks.

Carbon isotope values of the 55 samples range from -10.69‰ to 1.40‰. Late Jurassic samples have carbon isotope values ranging from -2.18‰ to 0.38‰. Late Jurassic to Cretaceous samples exhibit carbon isotope values from -1.14‰ to 0.42‰. Cretaceous samples have carbon values from -10.69‰ to 0.85‰, Late Cretaceous to Eocene samples have carbon values from -9.56‰ to -5.12‰. Neogene samples range from -7.64‰ to -5.69‰. The carbonate nodules from the Late Cretaceous to Eocene (sample 03LQ140-2) display the most negative $\delta^{13}C$ signature of the whole suite of rocks at -14.73‰.

Figure 4 shows sample $\delta^{18}O$ and $\delta^{13}C$ values as a function of their geologic age. Oxygen and carbon are plotted as 9-point running averages and major global climate periods are also shown on the diagram for comparison with the isotopic trends.

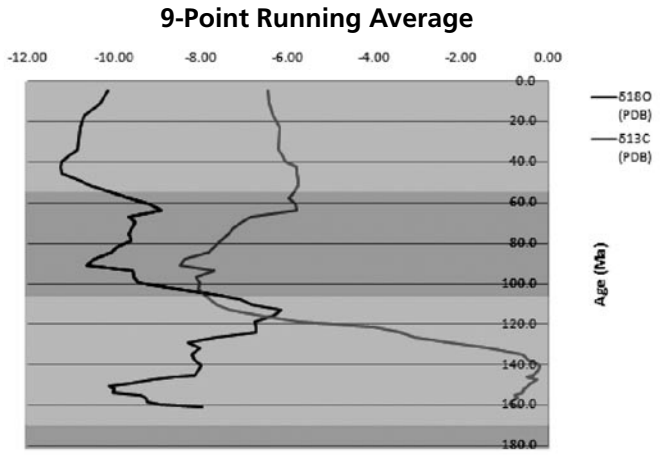

Figure 4: 9-point running average of $\delta^{18}O$ data (black line) and $\delta^{13}C$ data (red line). Shading indicates global climate periods. Pink represents warm periods, blue represents cool periods (Frakes, 1992; Vaughan, 2007; Wallmann, 2001).

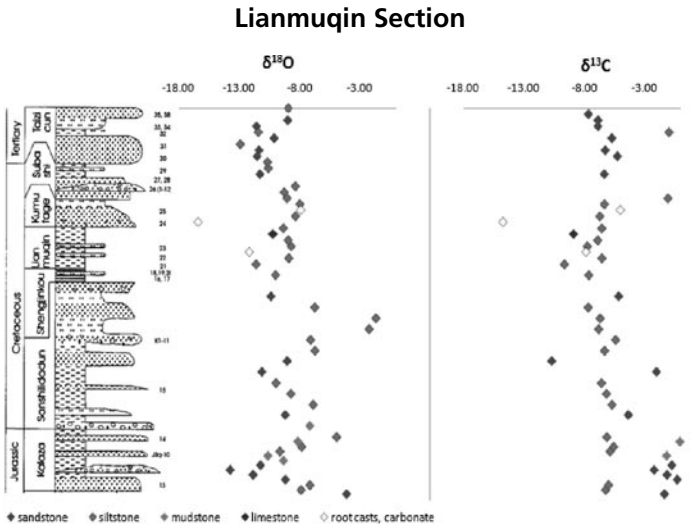

Figure 5: Stratigraphic column from the Lianmuqin Section sample locality plotted against the oxygen and carbon isotope data from this study (column modified from Shao et al., 1999).

Figure 5 shows oxygen and carbon values plotted against the stratigraphic column from the Lianmuqin Section where the rock samples were collected.

Discussion

Taking the overall data given by the 55 sedimentary rock samples from the Turpan Basin into account, the inference can be made that the isotopic record can be viewed as three separate signals: two in response to tectonic influences sandwiched between a period where climate dominates.

Possible influences on the isotopic record including detrital effects, diagenesis, and climate, can alter oxygen and carbon values. Due to the interaction of calcite with meteoric waters at high temperatures, diagenesis can result in exceptionally low oxygen isotope values (Dickson and Coleman, 1980). Detrital processes can contaminate samples with carbonate from unknown origins.

The Late Cretaceous (90-65 Ma) $\delta^{18}O$ and $\delta^{13}C$ data track together suggesting that evaporation may have altered the isotope record during this time in a possible climate dominated signal. This climate dominated signal is consistent with the warm and highly arid climate of the Mesozoic (Takashima et al., 2006) along with high P_{CO2} levels during this time (Ekart et al., 1999) causing the signature of atmospheric carbon to be significant in the record (Cerling, 1984). The Late Jurassic and Early Cretaceous (160-110 Ma) and Tertiary (<65 Ma) $\delta^{18}O$ and $\delta^{13}C$ data do not track together inferring a cause unrelated to climate. The opposing oxygen and carbon signals during the Late Jurassic and Early Cretaceous periods could be the result of the tectonic Jurassaic inception of the Turpan Basin described in models supported by stratigraphic and plaeocurrent data (Hendrix et al., 1992; Grenne et al., 2001; Greene et al., 2005). The Tertiary data also exhibits a similar divergent oxygen and carbon trend. Tertiary samples present in this study are from a conglomerate giving a greater chance that their values were increased by detrital marine carbonate. However, this change to a more high energy sedimentary environment suggests that this is when uplift was rapidly occurring, coinciding with India's collision into Eurasia (Tapponnier et al., 2001). These results are consistent with a two stage uplift senario for the Bogda Shan beginning with the formation of the Turpan Basin in the Jurassic and ending with a second uplift event during the early Tertiary.

The goal of this research was to define paleoelevations and paleoclimates using stable isotopes. However, uncertainties exist. The Tibetan Plateau exhibits some of the most extreme atmospheric circulation patterns and tectonic arrangements on Earth. It is thought that a combination of climate effects and tectonic uplift has resulted in the Bogda Shan's intricate isotopic record. This research is being continued and future work will help to better understand the complex history of the Bogda Shan.

Acknowledgements

I would like to thank Bradley Ritts and Yongjun Yue for providing the samples necessary to do this research, along with Malinda Kent-Corson for her initial involvement. I appreciate Peter Blisniuk's help and dedication with the mass spectrometer at Stanford University's Stable Isotope Biochemistry Laboratory. I greatly value the support and thoughtful reviews of Robert Cicerone and Peter Saccocia. Financial support for this research was provided by Bridgewater State University's Adrian Tinsely Program and a Geological Society of America's Northeastern Section student research grant.

References

Cao, C.Z., 1990, The plate tectonic of northern Xinjiang, northwest China: Shenyang Institute of Geology and Mineral Resources, Bulletin, Chinese Academy of Geological Sciences, no.22, p. 26–32 (in Chinese). *in* Shao, L., et al., 2001. Sandstone Petrology and Geochemistry of the Turpan Basin (NW China): Implications for the Tectonic Evolution of a Continental Basin, Journal of Sedimentary Research, vol. 71, No. 1, p. 37-39.

Carroll, A.R., Liang, Y.H., Graham, S.A., Xiao, X.C., Hendrix, M.S., Chu, J.C., and McKnight,C.L., 1990, Junggar Basin, Northwest China: trapped late Paleozoic Ocean: Tectonophysics. v. 181, p. 1–14.

Carroll, A.R., Graham, S.A., Hendrix, M.S., Chu, J.C., McKnight, C.L., Feng, Y.M., Liang,Y.H., Xiao, X.C., Zhao, M., Tang, Y.Q., Li, J.Y., and Zhu, B.Q., 1991, Characteristics of sedimentation in Late Paleozoic Junggar basin and its basement,

Cerling, T.E., 1984, The stable isotopic composition of modern soil carbonate and its relationship to climate, Earth and Planetary Science Letters, vol. 71, p. 229-240.

Chen, Z.F., 1985, 1:20,000,000 Geologic Map of Xinjiang Uygur Autonomous Region, China, Geological Publishing House, Beijing.

Currie, B.S., Rowley, D.B., Tabor, N.J., 2005, Middle Miocene Paleoaltimetry of southern Tibet:implications for the role of male thickening and delamination in the Himalayan orogen, Geology, vol. 33, p. 181-184.

Cyr, A., Currie, B.S., Rowley, D.B., 2005, Geochemical and stable isotopic evolution of Fenghuoshan Group lacustrine carbonates, north-central Tibet: implications for the Paleoaltimetry of Late Eocene Tibetan Plateau, Geology, vol. 113, p. 517-533.

DeCelles, P.G., Quade, J., Kapp, P., Fan, M., Dettman, D.L., Ding, L., 2007, High and dry in central Tibet during the Late Oligocene, Earth and Planetray Science Letters, vol. 253, p. 389-401 .

Ding, D.G., Tang, L.J., Qian, Y.X., Liu, W.X., Lu, X.B., Cui, K.R., Wang, D.X., Gao, C.L., Sha, Q.L., Shi, Y., and Sun, S.Q., 1996, Formation and evolution of the Tarim basin: Nanjing, China, Hehai University Press, 302 p. (in Chinese with English abstract). *in* Shao, L., et al., 2001. Sandstone Petrology and Geochemistry of the Turpan Basin (NW China): Implications for the Tectonic Evolution of a Continental Basin, Journal of Sedimentary Research, vol. 71, No. 1, p. 37-39.

Dickson, J.A., Coleman, M.L., 1980. Changes in carbon and oxygen isotopic composition during limestone diagensis, Sedimentology vol. 27, p. 107-118.

Ekart, D.D., Cerling, T.E., Montanez, I.P., Tabor, N.J., 1999, A 400 million year carbon isotope record of pedogenic carbonate: implications for paleoatmospheric carbon dioxide, American Journal of Science, vol. 299, p. 805-827.

Frakes, L.A., Francis, J.E., Syktus, J.I., 1992, Climate Modes of the Phanerozoic: The History of the Earth's Climate over the Past 600 Million Years, Cambridge University Press, Cambridge.

Greene, T.J., Carroll, A.R., Hendrix, M.S., Graham, S.A., Wartes, M.A., Abbink, O.A., 2001. Sedimentary record of Mesozoic deformation and inception of the Turpan-Hami basin, northwest China, Geological Society of America Memoir vol. 194, p. 317-340.

Green, T.J., Carroll, A.R., Wartes, M., Graham, S.A., and Wooden, J.L., 2005 Integrated Provenance Analysis of a Complex Orogenic Terrane: Mesozoic Uplift of the Bogda Shan and Inception of the Turpan-Hami Basin, NW China, Journal of Sedimentary Research, vol. 75, no. 2, p. 251-267.

Hendrix, M.S., Graham, S.A., Carroll, A.R., Sobel, E.R., McKnight, C.L., Schulein, B.J., and Wang, Z., 1992 Sedimentary record and climate implications of the recurrent deformation in the Tian Shan: evidence from Mesozoic strata of north Tarim, south Junggar, and Turpan basins, northwest China: Geological Society of America Bulletin, vol. 105, p. 53-79.

Hu, J.Y., Zhao, W.Z., Qian, K., Li, X.D., and Li, Q.M., 1996, Fundamental characteristics of petroleum geology in NW China: Acta Petrolei Sinica, v. 17, p. 1–11 (in Chinese with English abstract). *in* Shao, L., et al., 2001. Sandstone Petrology and Geochemistry of the Turpan Basin (NW China): Implications for the Tectonic Evolution of a Continental Basin, Journal of Sedimentary Research, vol. 71, no. 1, p. 37-39.

Kent-Corson, M.L., Ritts, B.D., Zhuang, G., Bovet, P.M., Graham, S.A., Chamberlain, C.P., 2009. Stable isotopic constraints on the tectonic, topographic, and climatic evolution of the northern margin of the Tibetan Plateau, Earth and Planetary Science Letters vol. 282, p. 158-166.

Li, W.H., 1997a. Sequence stratigraphy of Jurassic in Taibei Sag, Turpan-Hami Basin (in Chinese with English abstract). Oil Gas Geol. 3 (18), 210–215.

Li, W.H., 1997b. Wenjisang braid delta in Taibei Sag, Turpan-Hami Basin and its hydrocarbon accumulation (in Chinese with English abstract). Oil Gas Geol. 3 (18), 231–235. *in* Shao, L., Stattegger, K., LI, W., and Haupt, B.J., 1999, Depositional style and subsidence history of the Turpan Basin (NW China): Sedimentary Geology, vol. 128, p. 155–169.

Molnar, P., England, P., Martinod, J., 1993. Mantle dynamics, uplift of the Tibetan Plateau, and the Indian Monsoon, Reviews of Geophysics vol. 31, p. 357-396.

Poage, M.A., Chamberlain, C.P., 2001. Empirical relationships between elevation and the stable isotope composition of precipitation and surface waters: Considerations for studies of paleoelevation change, American Journal of Science vol. 301, p. 1-15.

Rowley, D.B. Currie, B.S., 2006. Palaeo-altimetry of the late Eocene to Miocene Lunpola Basin, central Tibet, Nature, vol. 439, p. 677-681.

Rowley, D.B., Garzione, C.N., 2007, Stable Isotope-Based Paleoaltimetry, Annual Review of Earth and Planetary Sciences, vol. 35, p. 463-508

Shao, L., Stattegger, K., LI, W., and Haupt, B.J., 1999, Depositional style and subsidence history of the Turpan Basin (NW China): Sedimentary Geology, vol. 128, p. 155–169.

Shao, L., Stattegger, K., Garbe-Schoenberg, CD., 2001. Sandstone Petrology and Geochemistry of the Turpan Basin (NW China): Implications for the Tectonic Evolution of a Continental Basin, Journal of Sedimentary Research, vol. 71, no. 1, p. 37-39.

Spicer, R.A., Harris, N.B.W., Widdowson, M., Herman, A.B., Guo, S., et al. 2003.Constant elevation of southern Tibet over the past 15 million years. Nature vol. 421, p. 622-624.

Takashima, R., Hiroshi, N., Huber, B.T., Leckie, R.M, 2006, Greenhouse World and the Mesozoic Ocean, Oceanography, vol. 19, no. 4, p. 82-92.

Tapponnier, P., Zhiqin, X., Roger, F., Meyer, B., Arnaud, N., Wittlinger, G., Jingsui., 2001, Oblique Stepwise Rise and Growth of the Tibet Plateau, Science's Compass Review, vol. 294, p. 1671-1677.

Vaughan, A.P.M., 2007. Climate and geology – a Phanerozoic perspective. *in* Williams, M., Haywood, A.M., Gregory, F.J. and Schmidt, D.N. (eds) Deep-Time Perspectives on Climate Change: Marrying the Signal from Computer Models and Biological Proxies. The Micropalaeontological Society, Special Publications. The Geological Society, London, 5–60.

Wallmann, K., The Geological Water Cycle and the Evolution of Marine $\delta^{18}O$ Values, Geochimica et Cosmochimica Acta, vol. 65, no. 15, p. 2469-2485.

Wu, T., Zhao, W.Z., 1997. The Formation and Distribution of Coal-Bearing Oil Fields in Turpan Basin (in Chinese). Petroleum Industry Publishing House, Beijing, 271 pp. *in* Shao, L., Stattegger, K., LI, W., and Haupt, B.J., 1999, Depositional style and subsidence history of the Turpan Basin (NW China): Sedimentary Geology, vol. 128, p. 155–169.

Zhu, X., Yang, H., 1988. Evolutionary characteristics of intermontane coal basins of the Mesozoic and Cenozoic basins in Tianshan (in Chinese with English abstract). Xinjiang Geol. 6, 83–91. *in* Shao, L., Stattegger, K., LI, W., and Haupt, B.J., 1999, Depositional style and subsidence history of the Turpan Basin (NW China): Sedimentary Geology, vol. 128, p. 155–169.